Optical Fingerprints of Si Honeycomb Chains and Atomic Gold Wires on the Si(111)-(5 × 2)-Au Surface

Conor Hogan,[1,2,*] Elena Ferraro,[2,3] Niall McAlinden,[4,5] and John F. McGilp[4]

[1]*CNR-Istituto di Struttura della Materia, via Fosso del Cavaliere 100, 00133 Rome, Italy*
[2]*European Theoretical Spectroscopy Facility (ETSF) and Dipartimento di Fisica, Università di Roma "Tor Vergata," Via della Ricerca Scientifica 1, 00133 Roma, Italy*
[3]*Laboratorio MDM, IMM-CNR, Via Olivetti 2, I-20864 Agrate Brianza, Italy*
[4]*School of Physics, Trinity College Dublin, Dublin 2, Ireland*
[5]*Institute of Photonics, SUPA, University of Strathclyde, Glasgow G4 0NW, United Kingdom*

(Received 6 March 2013; revised manuscript received 25 June 2013; published 22 August 2013)

The intensively studied Si(111)-(5 × 2)-Au surface is reexamined using reflectance anisotropy spectroscopy and density functional theory simulations. We identify distinctive spectral features relating directly to local structural motifs such as Si honeycomb chains and atomic gold wires that are commonly found on Au-reconstructed vicinal Si(111) surfaces. Optical signatures of chain dimerization, responsible for the observed (×2) periodicity, are identified. The optical response, together with STM simulations and first-principles total-energy calculations, exclude the new structure proposed very recently based on the reflection high-energy electron diffraction technique analysis of Abukawa and Nishigaya [Phys. Rev. Lett. **110**, 036102 (2013)] and provide strong support for the Si honeycomb chain with the triple Au chain model of Erwin *et al.* [Phys. Rev. B **80**, 155409 (2009)]. This is a promising approach for screening possible models of complex anisotropic surface structures.

DOI: 10.1103/PhysRevLett.111.087401 PACS numbers: 78.68.+m, 73.20.−r, 78.20.Bh

The Si(111)-(5 × 2)-Au surface has been the subject of long and intensive experimental and theoretical study, due to its potential for applications in nanoelectronics and its prototypical nature for studying self-assembly and properties of one-dimensional quantum structures [1,2]. On the experimental side, this includes STM [3–5], reflection high-energy electron diffraction (RHEED) [6], LEED [7], photoemission [8–10], and optical spectroscopy [11,12]; theoretical works generally focus on surface energies, electronic structure, and STM simulations [13–16]. Nonetheless, its structure remains controversial. Significant inconsistencies arose when even the most promising structures, all of which feature a Si honeycomb chain [17], were compared with experimental data [5].

The recalibration in 2009 [18] of the Au coverage from 0.4 monolayers (ML) to 0.6 ML prompted a reevaluation of the Si(111)-(5×2)-Au atomic structure. In particular, an exhaustive theoretical-experimental study by Erwin-Barke-Himpsel [16] (henceforth, EBH) proposed a three-chain model that largely resolved the remaining discrepancies in the STM and photoemission data [5]. However, a recent RHEED study by Abukawa and Nishigaya [6] (henceforth, AN) predicted a completely new structure, which appears consistent with *Y*-shaped structures found in STM [3,5]. Most notably, the model does not contain Si honeycomb chains.

Independent evaluation of competing structural models is provided by reflectance anisotropy spectroscopy (RAS) [19]. The technique probes both filled and empty surface and interface states while discriminating against the bulk response of cubic materials and hence is particularly sensitive to the local surface and interface atomic structure. Moreover, RAS simulation has now evolved to a level capable of producing impressive agreement with experiment, revealing sensitivity to subtle structural phenomena, such as dimer composition [20] and buckling angle [21], structural isomerism [22] and subsurface defects [23], as well as adsorption geometry [24], kinetics [25], and electronegativity [26] in interface systems. Adsorbate-reconstructed Si(111) and vicinal Si(*hhl*) surfaces are particularly sensitive to RAS due to the richness of highly anisotropic structural elements that form by self-assembly during surface preparation [8,12]. A recent study of quasi-1D indium chains on Si(111) highlighted the power of a combined theoretical-experimental optical spectroscopy study of these kinds of systems [22].

In combination with simulations of STM images and *ab initio* total-energy calculations, we compute RAS spectra of the various proposed models of Si(111)-(5 × 2)-Au and compare our results with previously measured spectra [12]. The evidence clearly supports the EBH model over the recently proposed AN structure. We confirm the presence of distinctive structural motifs like Si honeycomb chains and Au atomic chains, and show that their spectral fingerprints are present in another well-known Au-stabilized vicinal surface. We also examine the role of adatoms in stabilizing the surface chains and find evidence consistent with a charge transfer mechanism between separate microdomains on the experimentally prepared Si(111)-(5 × 2)-Au surface.

Structural optimizations were performed using density functional theory in the local density approximation (DFT

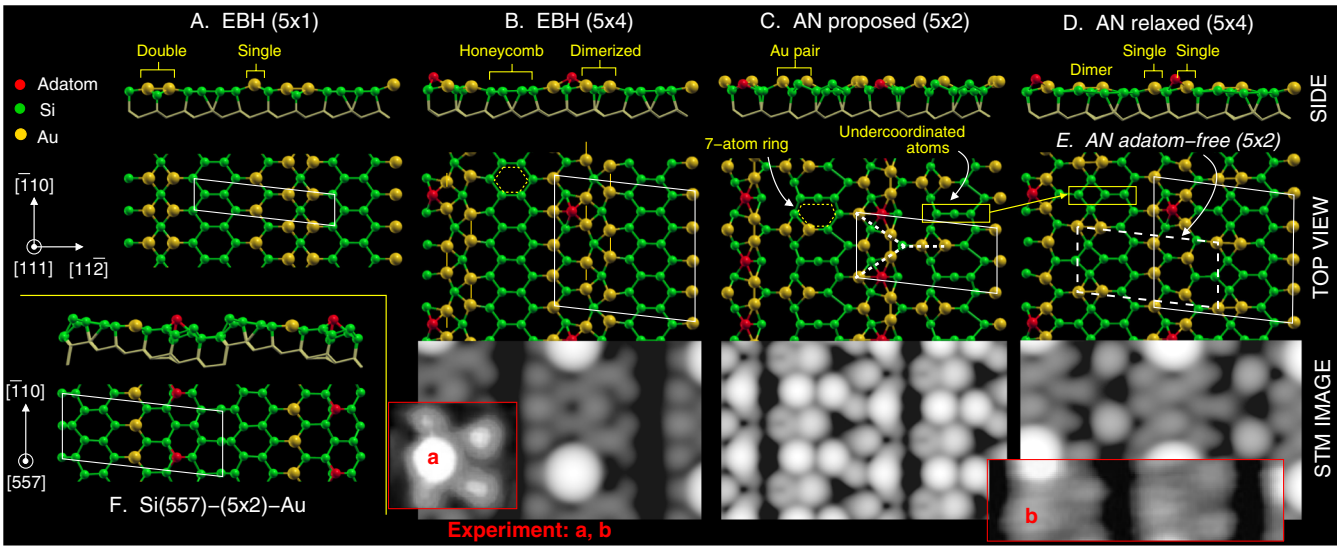

FIG. 1 (color online). Structures (top layers only) and simulated STM images of proposed models for Si(111)-(5 × 2)-Au at a 0.6 ML Au coverage. Surface unit cells are indicated by the solid (white) lines, except for model *E* (dashed line), which is shown as a subsection of model *D*. The single-chain model of Si(557)-(5 × 2)-Au is also shown (*F*). Constant current STM images are calculated at a bias of −1.0 eV. Partial experimental images extracted from (a) Ref. [5] and (b) Ref. [4] at biases of −0.4 and −1.5 eV, respectively.

LDA) [27], within a plane-wave [28] and norm-conserving pseudopotential [29] framework. Surfaces were modeled using supercells containing thin slabs of six double layers of Si, backterminated with hydrogens and separated by vacuum regions about 14 Å thick. A kinetic-energy cutoff of 50 Ry was assumed along with equivalent 4 × 4 and 4 × 2 **k**-point meshes for (5 × 2) or (5 × 4) cells, respectively, and a Gaussian smearing of 0.1 eV was used. Surface energies were checked using the Perdew-Burke-Ernzerhof functional modified for solids (PBEsol) [30] within the projector-augmented-wave method [31]. Although relativistic pseudopotentials are used for Au, spin-orbit coupling is neglected, as its effect on RAS has been shown to be minor (mostly causing some broadening) [23,32]. Further details of the approach can be found elsewhere [32]. Constant current STM images are computed from the local density of states using the Tersoff-Hamann approximation [33].

Proposed models of the Si(111)-(5 × 2)-Au surface at a 0.6 ML Au coverage are illustrated in Fig. 1, alongside the established model for Si(557)-(5 × 2)-Au. The EBH triple-chain undimerized (*A*) and adatom-dimerized (*B*) models and AN proposed (*C*), relaxed (*D*), and adatom-free (*E*) models are shown. Double chains in the basic EBH (5 × 1) cell (*A*) dimerize in the presence of adatoms, leading to a ×2 period doubling along the chain direction; the adatom superstructure produces the (5 × 4) unit cell (*B*). In contrast, the AN model features *Y*-shaped structures composed of Au atoms, which contains a Au-Au dimer oriented along $[\bar{1}10]$. Si adatoms bridge adjacent *Y* elements. The Si honeycomb chain is notably absent from *C*, its place taken by a $[11\bar{2}]$-oriented Au pair.

Our DFT calculations reveal that the AN model as proposed is structurally unstable. This is due to the presence of energetically unfavorable elements such as seven-atom Si rings and undercoordinated Si atoms (see Fig. 1). When we allowed the AN model to relax, these elements reconstruct to yield model C^* (Table I; not shown in Fig. 1), the adatom-free version of this being model *E*. The $[\bar{1}10]$ dimer (between the arms of the *Y*) breaks immediately upon relaxation, even in the presence of adatoms, in sharp contrast to the EBH model, where charge transfer from adatoms induces dimerization in the double chain [16]. On relaxation, the vertical atomic positions differ substantially from those predicted by RHEED.

Surface energies quantify the differing stability of these models. Table I reports computed surface energies with respect to model *A*, obtained using the standard expression $\Delta E_s = E_s - E_s^A - \Delta n_{\mathrm{Si}} \mu_{\mathrm{Si}}$. Here, E_s is the total energy of a particular model, Δn_{Si} is the number of Si atoms in excess of that in *A*, and μ_{Si} is the computed bulk Si chemical potential. Results from the different DFT functionals agree to within 3 meV. All models based on the *Y* structure, including the relaxed AN model (C^*, not shown)

TABLE I. Surface energies ΔE_s of Si(111)-(5 × 2)-Au structural models with respect to that of model *A*, computed within LDA and PBEsol. Values of ΔE_s are in eV/(1 × 1) cell. θ_{Si} is the coverage (in ML) of Si adatoms.

Model	θ_{Si}	LDA	PBEsol	Description
A (5 × 1)	0.00	+0.000	+0.000	EBH, triple chain
B (5 × 4)	0.05	−0.022	−0.020	EBH, with adatom
C (5 × 2)	0.10	>0.500	>0.500	AN, proposed
C^* (5 × 2)	0.10	+0.084	+0.081	AN, relaxed
E (5 × 2)	0.00	+0.089	+0.090	AN, adatom-free
D (5 × 4)	0.05	+0.085	+0.085	AN, relaxed

and the corresponding adatom-free case E, are energetically unstable even with respect to the basic EBH model A by $\sim$80 meV/(1 × 1) cell. A fourth model (D), constructed to have an adatom coverage of 0.05 ML, was also found to be unstable. The strength of A and B derives from the presence of the Si honeycomb chain, which is a stabilizing feature of metal-adsorbed Si(111)-(3 × 1) reconstructions [17] and vicinal Si(hhl)-Au surfaces [8,34], with further stability deriving from the adatom-induced dimerization of the double chains. Neither of these phenomena is present in the AN models.

STM simulations support these findings. Experimental measurements on Si(111)-Au report bright rows aligned along $[\bar{1}10]$ having a (× 4) or (× 2) periodicity at their edge and separated by thinner unbroken dark regions. The rows contain elongated Y-shaped elements or smaller V-shaped elements appearing symmetrically around bright protrusions. Typical sections at negative bias are shown in Fig. 1. We reproduced the previously reported simulated image for model B [16], which clearly identifies all key features: dark rows correspond to the honeycomb chains, bright spots are the adatoms, and other shapes derive from Au-Si bonds. In contrast, neither of the AN models succeeds in explaining the observed images, even though the original topology appears consistent with the reported Y-shaped elements: the positioning of bright features with respect to the adatoms is incorrect, and dark channels are narrowed (C) or interrupted by bright spots (D). This comparison highlights the danger of interpreting STM images from bare atomic positions without performing *ab initio* calculations of the local density of states.

Important new evidence in support of the EBH model comes from comparison of the measured and computed surface optical response. Because of the difficulty in preparing a single-domain nominal surface, spectra have been measured on vicinal surfaces. Data shown in Fig. 2 correspond to a vicinal Si(111)-Au surface offcut by 4° in the $[11\bar{2}]$ direction and are very similar to data from a sample offcut by 3° towards $[\bar{1}\,\bar{1}\,2]$. The step contribution was thus estimated to be small, with the 4° offcut closely resembling the extracted terrace response [12]. The RAS is expressed as $\Delta R/R = 2(R_{[\bar{1}10]} - R_{[11\bar{2}]})/(R_{[\bar{1}10]} + R_{[11\bar{2}]})$, where R_α is the reflectance of normal-incident light polarized along a direction α in the surface plane. Theoretical spectra were calculated within DFT LDA at the independent-particle level, with no adjustable parameters. Dense $\mathbf{k}$-point meshes [800 $\mathbf{k}$ points per (1 × 1) cell] were used. The response of the front surface was extracted using a real-space cutoff function [35]. The theory axis is shifted by +0.4 eV in Fig. 2 to allow for the underestimation of the optical gap in the DFT LDA approach. The standard slab polarizability expression for RAS has a prefactor of $8\pi\omega/c$ [36], and applying a scissors operator of +0.4 eV to produce this shift would increase the RAS peak intensities by $0.4/\omega$ (40% at 1.0 eV and 16% at 2.5 eV), improving agreement with experiment. The supercell size inhibits the use of more advanced methods that account for self-energy and excitonic effects.

Experiment shows that the real surface is of mixed microdomain character [9,16,37], but we start by considering the optical signal of a simple single domain. The RAS response for the original AN model (C), the relaxed (5 × 4) AN model (D), and the EBH model (B) are shown in Fig. 2(a). Some similarities exist among the computed spectra due to the presence of several common structural motifs: Au-Si-Au chains along $[\bar{1}10]$, Au-Au dimers along $[11\bar{2}]$, and adatoms. Nonetheless, the best overall agreement with experiment is given by model B. From 1.3 to 3.2 eV, models C and D have only half the intensity of model B. While the opposite is the case for the low-energy peak from 0.4 to 1.3 eV, this has only half the energy range, and, in addition, the experimental intensity (but not the

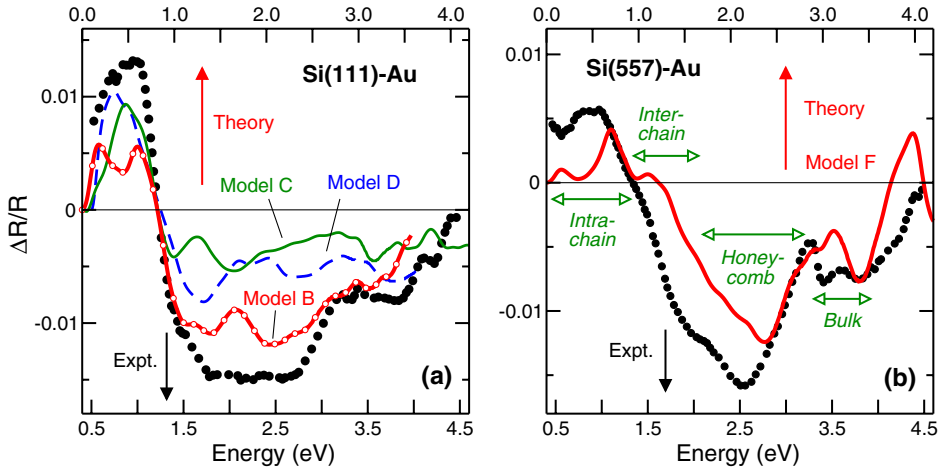

FIG. 2 (color online). Measured (solid black dots) and computed (lines) RAS response for Si(111)-(5 × 2)-Au (left panel) and Si(557)-(5 × 2)-Au (right panel). The experimental data are taken from Ref. [12]. Labels refer to structural models in Fig. 1. Note the rigid shift in the energy axis between theory and experiment.

shape or position) of the low-energy peak varies from sample to sample [12].

A more detailed interpretation of the spectral line shape strengthens this conclusion. The computed RAS response of Si(557)-(5 × 2)-Au is shown in Fig. 2(b) and compared with the available experimental data [12,38]. Like Si(111)-Au, the Si(557)-Au surface has been the subject of intensive study over the last decades, and as a result its structure is well known [2,39]. As shown in Fig. 1 (model *F*), it comprises single Au chains aligned along $[\bar{1}10]$ with Si honeycomb chains present at the step edge. The agreement in Fig. 2(b) is very good, providing an independent confirmation of this single-chain model. Comparison of Figs. 2(a) and 2(b) reveal that the major difference between the two Au-reconstructed systems is the additional strong negative signal between 1.5 and 2.0 eV in the Si(111)-Au case.

Analysis of the single-particle transitions in each case reveals that the broad negative peak between 2.0 and 3.2 eV is a signature of the Si honeycomb chains present in both systems. Although the chains themselves run along $[\bar{1}10]$, the optical peak is due to localized transitions along the $[11\bar{2}]$ direction between filled and empty states on the honeycomb edge atoms and central (double) bonds, respectively, giving a negative signal. The good agreement between theory and experiment for both systems in this energy range is a strong argument for the presence of these honeycombs in Au-reconstructed Si(111) and Si(*hhl*) surfaces. In the AN models, they are either absent (*C*) or contain Au atoms (*D*), with the result that the RAS response in this range is significantly reduced.

The remainder of the RAS spectra emanates from the Au chains. Briefly, the low-energy peak arises from intrachain transitions involving states delocalized along single or double chains, consistent with the positive sign of the RAS peak. Positive peaks in this spectral region have been identified previously with intrachain transitions for In chains on Si(111) [22]. The strong negative signal between 1.5 and 2.0 eV in the Si(111)-Au spectra derives from interchain (single-to-double) transitions, predominantly associated with Si-Au bonds oriented along $[11\bar{2}]$. The Au chains do not contribute to the RAS spectra in a completely straightforward manner, with the nature of the Au-surface bonding playing an important role. The small signal from the single chain Si(557)-Au structure is consistent with the absence of adjacent chains to support such transitions.

The identification of anisotropic structural motifs at these surfaces, which generate distinct signals in the optical spectra, opens the way to using these optical fingerprints to search for new structural models, as well as testing the validity of proposed ones [e.g., Si(553)-Au [40] and Si(775)-Au [8]]. The numerous degrees of freedom involved in exploring large reconstructed or stepped surfaces makes the search for the correct model particularly difficult. Systematic total-energy simulations [15], Monte Carlo methods [41], and even genetic algorithms [42]—all of which require intensive computational resources—are appearing more frequently. RAS may offer significant advantages in the search for new models of anisotropic surface structures.

RAS is sensitive to quite subtle structural distortions within the Au chains, for example, the dimerization of the double Au chain responsible for the observed ×2 periodicity [9]. In Fig. 3, we compare the optical spectrum of the undimerized model *A* to that of two models having dimerized chains. As demonstrated by EBH, this occurs either through the presence of one adatom per (5 × 4) cell (model *B*) or by explicit "doping" with electrons [1*e* per (5 × 2) cell]. While the undimerized model shows only a weak, flattish structure around 0.3 eV, both dimerized surfaces show similar well-defined positive peaks near 0.6 eV in the dimer bond direction. The overall similarity of the doped (5 × 2) and full (5 × 4) spectra suggests that the stabilizing effect of adatom coverage can be modeled without having to use larger surface cells, in agreement with previous work [13].

This observation allows us to return, finally, to the real Si(111)-(5 × 2)-Au surface, which has a global adatom coverage of 0.025 ML, i.e., *half* that of model *B* [4,9,10]. Reports indicate that the surface is split into microdomains of adatom-free regions and (5 × 4)-reconstructed regions [9,16,37]; evidence of charge transfer from adatoms has been presented [5]. We confirmed explicitly that if adatoms are present, dimerization of the double chain remains even if two electrons are removed from the (5 × 4) cell and the surface allowed to relax (i.e., the ×2 periodicity persists). This implies that the charge donated from the adatoms is still retained by the double chains. An approximate RAS response of the mixed-domain surface can thus be estimated from an average of the positively charged (5 × 4) signal and the negatively charged (5 × 2) cell, as shown in Fig. 3. While the overall spectrum shows only slightly better agreement with experiment, the low-energy line

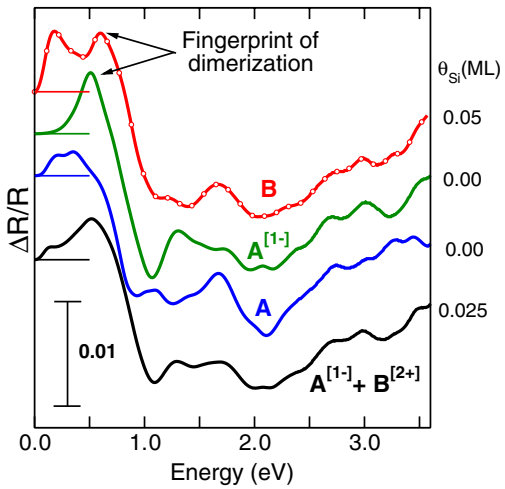

FIG. 3 (color online). Optical signatures of chain dimerization in Si(111)-Au. Square brackets indicate artificial doping of the simulation cell [*A*, (5 × 2); *B*, (5 × 4)]. $A^{[1-]} + B^{[2+]}$ represents a mixed-domain signal. θ_{Si} denotes the adatom coverage.

shape is significantly improved by the filling in of the valley between the two peaks in model *B*. The overall shape and intensity may of course be further modified by inclusion of excitonic effects and by inhomogeneity along the chains [12,37]. Nonetheless, the calculations are consistent with the presence of two charged microdomains at the Si(111)-Au surface.

In summary, surface energies, STM simulations, and RAS calculations allow the recently proposed AN model to be excluded in favor of the EBH triple-chain model. In addition, the combined experimental-theoretical approach to understanding the optical response has identified anisotropic structural motifs at these surfaces, which generate distinct signals in the optical spectra. This optical fingerprint approach is very promising for screening possible models of these important, but complex, anisotropic surface structures.

Financial support through the EU e-I3 ETSF Project No. 211956 (User Project 212), Science Foundation Ireland Grant No. 11/RFP/PHY3047, and the Irish Research Council for Science, Engineering and Technology (IRCSET) is acknowledged, as well as high performance computing resources and support from CINECA (ISCRA award SIMPLEX, 2011-2012). M. Oliveira is thanked for help in generating the Au pseudopotentials using the APE code [29].

*conor.hogan@roma2.infn.it

[1] F. J. Himpsel, K. N. Altmann, R. Bennewitz, J. N. Crain, A. Kirakosian, J.-L. Lin, and J. L. McChesney, J. Phys. Condens. Matter **13**, 11 097 (2001).
[2] I. K. Robinson, P. A. Bennett, and F. J. Himpsel, Phys. Rev. Lett. **88**, 096104 (2002).
[3] J. D. O'Mahony, C. H. Patterson, J. F. McGilp, F. M. Leibsle, P. Weightman, and C. F. J. Flipse, Surf. Sci. Lett. **277**, L57 (1992).
[4] A. Kirakosian, J. Crain, J.-L. Lin, J. McChesney, D. Petrovykh, F. Himpsel, and R. Bennewitz, Surf. Sci. **532–535**, 928 (2003).
[5] H. S. Yoon, J. E. Lee, S. J. Park, I.-W. Lyo, and M.-H. Kang, Phys. Rev. B **72**, 155443 (2005).
[6] T. Abukawa and Y. Nishigaya, Phys. Rev. Lett. **110**, 036102 (2013).
[7] H. E. Bishop and J. C. Rivière, J. Phys. D **2**, 1635 (1969).
[8] J. N. Crain, J. L. McChesney, F. Zheng, M. C. Gallagher, P. C. Snijders, M. Bissen, C. Gundelach, S. C. Erwin, and F. J. Himpsel, Phys. Rev. B **69**, 125401 (2004).
[9] J. L. McChesney, J. N. Crain, V. Pérez-Dieste, F. Zheng, M. C. Gallagher, M. Bissen, C. Gundelach, and F. J. Himpsel, Phys. Rev. B **70**, 195430 (2004).
[10] W. H. Choi, P. G. Kang, K. D. Ryang, and H. W. Yeom, Phys. Rev. Lett. **100**, 126801 (2008).
[11] J. Jacob, N. McAlinden, K. Fleischer, S. Chandola, and J. F. McGilp, Phys. Status Solidi C **5**, 2569 (2008).
[12] N. McAlinden and J. F. McGilp, Europhys. Lett. **92**, 67 008 (2010).
[13] S. C. Erwin, Phys. Rev. Lett. **91**, 206101 (2003).
[14] S. Riikonen and D. Sánchez-Portal, Phys. Rev. B **71**, 235423 (2005).
[15] F.-C. Chuang, C.-H. Hsu, C.-Z. Wang, and K.-M. Ho, Phys. Rev. B **77**, 153409 (2008).
[16] S. C. Erwin, I. Barke, and F. J. Himpsel, Phys. Rev. B **80**, 155409 (2009).
[17] S. C. Erwin and H. H. Weitering, Phys. Rev. Lett. **81**, 2296 (1998).
[18] I. Barke, F. Zheng, S. Bockenhauer, K. Sell, V. Oeynhausen, K. Meiwes-Broer, S. Erwin, and F. Himpsel, Phys. Rev. B **79**, 155301 (2009).
[19] D. E. Aspnes, J. P. Harbison, A. A. Studna, and L. T. Florez, Appl. Phys. Lett. **52**, 957 (1988); V. Berkovits, I. Makarenko, T. Minashvili, and V. Safarov, Solid State Commun. **56**, 449 (1985).
[20] C. Hogan, E. Placidi, and R. Del Sole, Phys. Rev. B **71**, 041308 (2005).
[21] C. Violante, A. Mosca Conte, F. Bechstedt, and O. Pulci, Phys. Rev. B **86**, 245313 (2012).
[22] S. Chandola, K. Hinrichs, M. Gensch, N. Esser, S. Wippermann, W. G. Schmidt, F. Bechstedt, K. Fleischer, and J. F. McGilp, Phys. Rev. Lett. **102**, 226805 (2009).
[23] C. Hogan, R. Magri, and R. Del Sole, Phys. Rev. Lett. **104**, 157402 (2010).
[24] A. Hermann, W. G. Schmidt, and F. Bechstedt, J. Phys. Chem. B **109**, 7928 (2005).
[25] N. Witkowski, K. Gaál-Nagy, F. Fuchs, O. Pluchery, A. Incze, F. Bechstedt, Y. Borensztein, G. Onida, and R. Del Sole, Eur. Phys. J. B **66**, 427 (2008).
[26] C. Hogan, D. Paget, O. E. Tereshchenko, and R. Del Sole, Phys. Status Solidi C **2981**, 2976 (2003).
[27] J. P. Perdew and A. Zunger, Phys. Rev. B **23**, 5048 (1981).
[28] P. Giannozzi *et al.*, J. Phys. Condens. Matter **21**, 395502 (2009).
[29] M. J. T. Oliveira and F. Nogueira, Comput. Phys. Commun. **178**, 524 (2008).
[30] J. P. Perdew, A. Ruzsinszky, G. I. Csonka, O. A. Vydrov, G. E. Scuseria, L. A. Constantin, X. Zhou, and K. Burke, Phys. Rev. Lett. **100**, 136406 (2008).
[31] P. E. Blöchl, Phys. Rev. B **50**, 17 953 (1994).
[32] C. Hogan, N. McAlinden, and J. F. McGilp, Phys. Status Solidi B **249**, 1095 (2012).
[33] J. Tersoff and D. R. Hamann, Phys. Rev. B **31**, 805 (1985).
[34] S. Riikonen and D. Sánchez-Portal, Phys. Rev. B **76**, 035410 (2007).
[35] C. Hogan, R. Del Sole, and G. Onida, Phys. Rev. B **68**, 035405 (2003).
[36] F. Bechstedt, *Principles of Surface Physics* (Springer-Verlag, Berlin, 2003).
[37] H. S. Yoon, S. J. Park, J. E. Lee, C. N. Whang, and I.-W. Lyo, Phys. Rev. Lett. **92**, 096801 (2004).
[38] N. McAlinden and J. F. McGilp, J. Phys. Condens. Matter **21**, 474208 (2009).
[39] D. Sánchez-Portal and R. M. Martin, Surf. Sci. **532–535**, 655 (2003).
[40] M. Krawiec, Phys. Rev. B **81**, 115436 (2010).
[41] C. V. Ciobanu and C. Predescu, Phys. Rev. B **70**, 085321 (2004).
[42] R. M. Briggs and C. V. Ciobanu, Phys. Rev. B **75**, 195415 (2007).